Full title

Peripheral and central employment of acid-sensing ion channels during early bilaterian evolution

Short title

Role of ASICs in bilaterians

Authors

Josep Martí-Solans[1], Aina Børve[2], Paul Bump[3], Andreas Hejnol[2*], Timothy Lynagh[1*]

Affiliations

1. Sars International Centre for Marine Molecular Biology, University of Bergen, Bergen, Norway
2. Department of Biological Sciences, University of Bergen, Bergen, Norway
3. Hopkins Marine Station, Department of Biology, Stanford University, Pacific Grove, CA, USA

*Corresponding authors
tim.lynagh@uib.no
andreas.hejnol@uib.no

Abstract

Acid-sensing ion channels (ASICs) are membrane proteins that endow vertebrate neurons with fast excitatory responses to decreases in extracellular pH. Although previous studies suggest that ASICs are found in certain invertebrates, the lineage in which ASICs emerged and the functional role of ASICs beyond the vertebrates is unknown. We reconstructed ASIC evolution by surveying metazoan ASICs and performing a phylogenetic analysis, which suggests that ASICs evolved in an early bilaterian. This was supported by electrophysiological measurements of proton-gated currents at heterologous channels from diverse bilaterians. This also revealed substantial variation in biophysical properties of broadly related ASICs, with selective sodium/potassium ion permeability ranging from 3- to 36-fold and half-maximal activating pH from 4.2 to 8.1. Furthermore, we studied the expression of ASICs in species outside the vertebrates and found expression in the central nervous system of certain bilaterian lineages but in the periphery, including nervous system, digestive system, and motile ciliated epithelia, of most lineages. The loss of such epithelial cells in Ecdysozoa might explain the loss of ASICs from this major animal lineage. Our results suggest that ASICs emerged in an early bilaterian, and expression in the central nervous system was accompanied or even pre-dated by expression in the periphery.

Introduction

Much of the morphological and behavioral complexity of animals is enabled by nervous systems in which neurons in the periphery sense and convey information from the environment, and more central neurons integrate and dispatch information to effectors [1, 2]. Such rapid sensory (environment → cell) and synaptic (cell → cell) signals rely on ligand-gated ion channels (LGICs), membrane proteins that convert chemical messages into ionic currents within milliseconds [3, 4]. These channels are found in all multicellular animals (Metazoa) and even in outgroup lineages such as bacteria and plants [5-7]. However, animals with nervous systems (Ctenophora, Cnidaria, and Bilateria) present a larger and more diverse LGIC gene content - i.e., more Cys-loop receptors, ionotropic glutamate receptors, and degenerin/epithelial sodium channel (DEG/ENaC) genes - than animals without nervous systems (Porifera and Placozoa) [8]. Although the evolution of the original nervous system(s) did not necessarily involve a rapid expansion of LGICs, the elaboration and refinement of nervous systems within particular lineages did, and this likely endowed bilaterian neurons with a sophisticated chemo-electrical toolbox in the ancestors of today's complex bilaterian animals [1, 8, 9]. Unfortunately, studies addressing the functional contribution of LGICs to early bilaterians are lacking [10].

Within the DEG/ENaC family of voltage-insensitive sodium channels, several independent expansions of neuronally expressed subfamilies have occurred, including degenerin channels (DEGs) in nematodes, pickpocket channels (PPKs) in arthropods, peptide-gated channels (HyNaCs) in cnidarians, and acid-sensing ion channels (ASICs) in vertebrates [11-15] (Fig 1A). ASICs are proton-gated ion channels that in rodents are widely expressed in the nervous system, with scattered expression in other cells, such as epithelia [16] (Fig 1B,C). In rodents and humans, ASICs are expressed or stimulus-upregulated in sensory neurons innervating skin, joints, and the gastrointestinal tract where their activation by acid or other inflammatory stimuli mediates touch or causes pain or hyperalgesia [17-20], typifying a chemosensory role. More recent experiments in rodents show that ASICs expressed postsynaptically in central neurons mediate depolarization in response to brief drops in synaptic pH during neurotransmission [21, 22], and ASICs thus perform an additional central role, mediating excitatory signals between neurons. Such roles might extend beyond the vertebrates, however, as it was recently discovered that functional ASICs exist in all Deuterostomia members (tunicates, cephalochordates, hemichordates and echinoderms), indicating that the ASIC subfamily is older than previously thought [12]. As ASICs are expressed in both central and peripheral neurons of tunicates [12, 23] and in sensory

neurons of echinoderms [24] (Fig 1B), it is difficult to assess the functional role of ASICs in early deuterostomes before they diversified.

It also remains unclear whether the ASIC subfamily might have emerged much earlier than the first deuterostomes and subsequent centralization of their nervous system, and what original function ASICs might have fulfilled earlier in metazoan evolution. Resolving this would require better resolution of the phylogenetic origin of ASICs. Furthermore, investigation of the expression of ASICs in a broader selection of species is required to address the evolution of peripheral, sensory and central, synaptic roles. We therefore performed a thorough phylogenetic investigation of metazoan DEG/ENaC genes, with a focus on ASICs, using unexplored transcriptomes and genomes. Moreover, we carried out expression analysis by in situ hybridization and determined the electrophysiological properties of several diverse ASICs from phylogenetically informative species. Results from these experiments enable a new hypothesis on the evolution and function of ASICs.

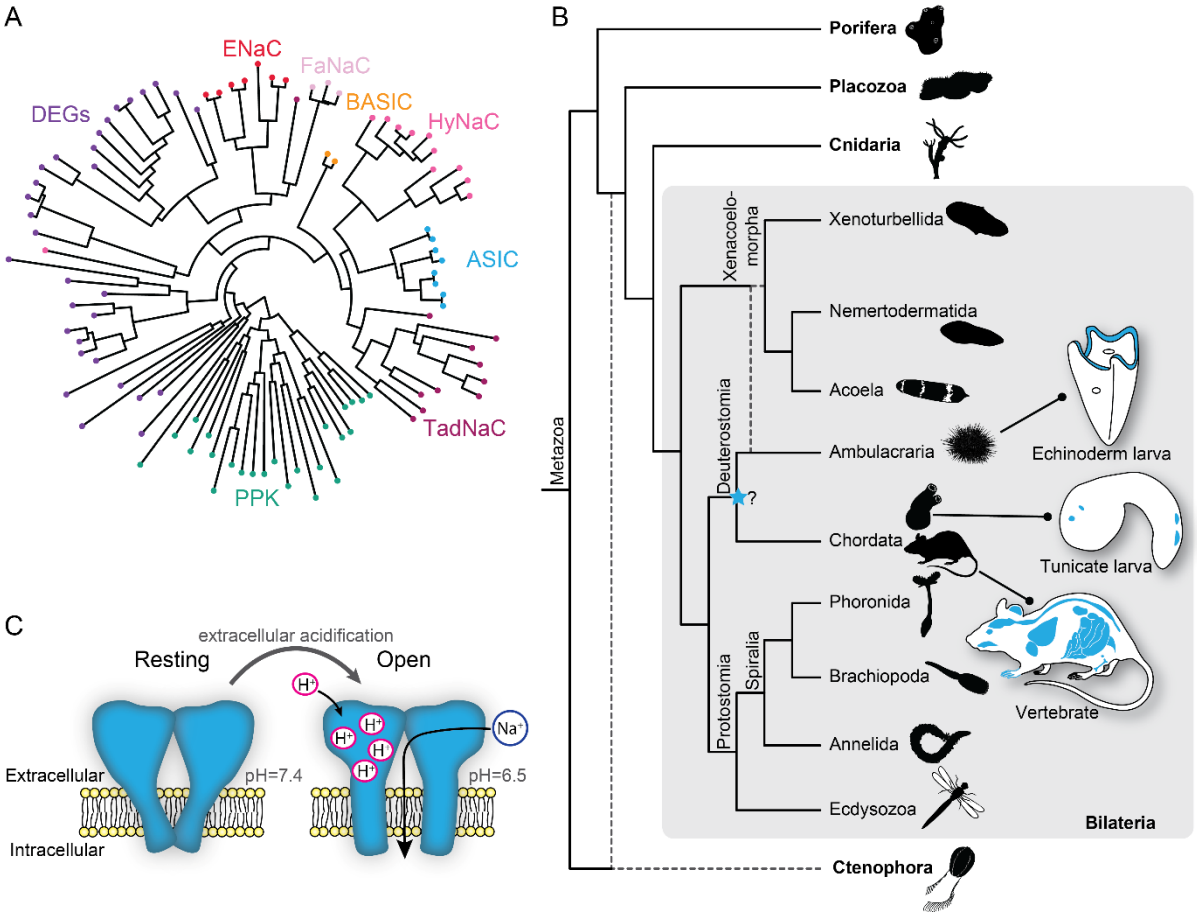

Fig 1. Overview of ASICs in Metazoa. (A) Abridged phylogenetic tree of the DEG/ENaC family showing major expansions of previously studied members (after [11, 25]). (B) Phylogenetic tree of main animal groups highlighting known ASIC expression (blue) and previously suggested ASIC emergence (blue star). Dotted lines show alternative positions for Ctenophora and Xenacoelomorpha. Cartoons show previously described ASIC protein and/or RNA expression in Chordata (rodent brain, spinal cord, lung, heart, kidney, gut, bladder, testis, bone, eye, ear, and skin [26]; tunicate larva sensory vesicle and bipolar tail neurons [23]) and Ambulacraria (echinoderm larva ciliary band [24]). (C) ASIC function. At rest, the channel is closed and impermeable. Upon extracellular acidification, certain amino acid side chains in the ASIC extracellular domain are protonated, causing conformational changes that open the channel, allowing sodium ions to flow down their chemo-electric gradient across the membrane.

Results

Broader phylogenetic study identifies ASICs in Protostomia and Xenacoelomorpha

We first sought a definitive picture of how broadly ASIC genes are conserved throughout the five metazoan lineages of Bilateria, Cnidaria, Porifera, Placozoa, and Ctenophora. To this end we utilized previously unexplored transcriptomes combined with canonical resources to search for DEG/ENaC genes from all lineages. The phylogenetic analysis of these 700 sequences from 47 species shows a well-supported clade of ASICs (Fig 2 and S1 Fig). The ASIC branch consists of two sub-clades "A" and "B", both of which include bona fide ASICs from deuterostome bilaterians. No ASICs were identified in Cnidaria, Porifera, Placozoa, and Ctenophora.

In contrast to previous studies, we detected bona fide ASICs in protostome and xenacoelomorph bilaterians (Fig 2). These include putative ASICs from seven protostome species—the annelid *Owenia fusiformis*, the nemertean *Notospermus geniculatus*, the brachiopods *Terebratalia transversa*, *Novocrania anomala* and *Lingula anatina*, the phoronid *Phoronopsis harmeri*, the bryozoan *Membranipora membranacea*, and six xenacolomorph species, the acoels *Hofstenia miamia*, *Isodiametra pulchra*, *Convolutriloba macropyga*, and *Childia submaculatum*, and the xenoturbellans *Xenoturbella bocki* and *Xenoturbella profunda*. Our analysis also included the hemichordate *Schizocardium californicum*, whose ASIC groups with previously reported hemichordate and echinoderm ASICs [12], indicative of broad conservation of ASICs in ambulacrarians. This shows that ASIC genes are present in the three major bilaterian groups of deuterostomes, protostomes, and xenacoelomorphs and absent from all other lineages, suggesting that ASICs diverged from other DEG/ENaC genes after the Cnidaria/Bilateria split and before the Bilateria diversified.

Protostomes are divided into Spiralia (such as annelids, molluscs, brachiopods, and phoronids), and Ecdysozoa (such as the nematode *Caenorhabditis elegans* and arthropod *Drosophila melanogaster*) (Fig 1B). Notably, the ASIC clade includes no ecdysozoan genes, although our analysis included DEG/ENaC genes from the nematode *Pontonema vulgare*, the pan-arthropods *Centruroides sculpturatus* and *Daphnia pulex*, and priapulids *Priapulus caudatus* and *Halicryptus spinulosus*. We also see no putative ASICs in certain spiralians, including the molluscs *Acanthopleura granulata* and *Crassostrea gigas*, the platyhelminths *Prostheceraeus vittatus* and *Schmidtea mediterranea* and in certain xenacoelomorphs, including the nemertodermatids *Meara stichopi* and *Nemertoderma westbladi*. This analysis suggests that ASICs, although found throughout Bilateria, were lost in the lineage to the Ecdysozoa shortly after the Ecdysozoa/Spiralia split and also disappeared in certain other bilaterian lineages such as molluscs and nemertodermatids.

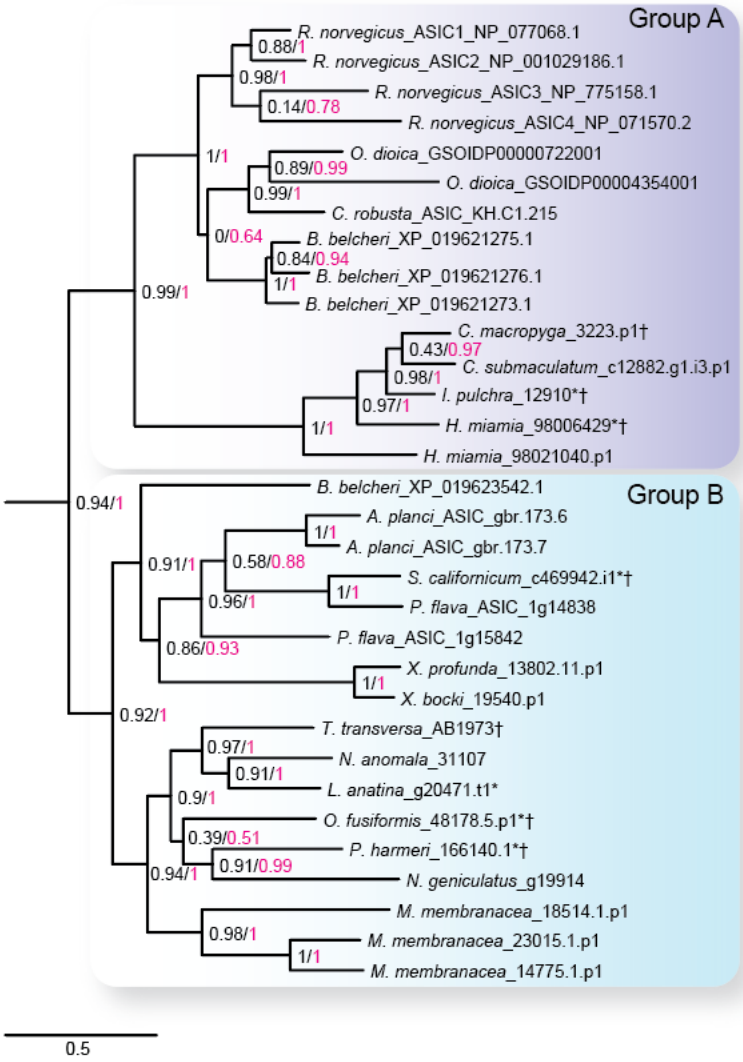

Fig 2. The ASIC branch of the DEG/ENaC family includes only bilaterian genes. ASIC branch from phylogenetic tree of DEG/ENaC family including 700 amino acid sequences from 47 metazoans (S1 Fig). Genes analyzed experimentally in this study are indicated by † (gene expression) and/or * (electrophysiology). Scale bar, amino acid substitutions per site. aLRT SH-like (black) and aBayes (magenta) likelihood-based support values indicated.

ASICs are expressed in two domains in Xenacoelomorpha

These results suggest that ASICs emerged during early bilaterian evolution, and we next sought evidence for potential biological roles by investigating the expression of ASIC genes in the different bilaterian lineages. The precise relationships between these lineages are under debate, but Xenacoelomorpha forms a putative sister group to all remaining Bilateria [27-30]. Therefore, we investigated ASIC expression in Xenacoelomorpha, utilizing the acoels *Isodiametra pulchra*, *Hofstenia miamia*, and *Convolutriloba macropyga*. Xenacoelomorphs show a large variation in nervous system architecture, but all possess a basal epidermal nerve plexus and some species, more internally, an anterior condensation of neurons or "brain" [31]. *I. pulchra* and *C. macropyga* also possess longitudinal bundles of neurons [32-34]. External to this nervous system in acoels is generally a sheet of longitudinal and ring muscles and, more externally, ciliated epithelial cells mediating locomotion [35-37].

From a dorsal view, expression of *I. pulchra* ASIC mRNA can be detected in several cells across the central anterior of the adult animal (Fig 3A). This is the location of the *I. pulchra* brain, where e.g.

serotonergic and peptidergic neurons form lateral lobes, connected by a frontal ring and a posterior commissure, and from which four pairs of nerve cords extend posteriorly (Fig 3A [32]). Fluorescent confocal micrographs show that the ASIC-expressing cells are associated with the posterior commissure of the brain and the dorsal and lateral neurite bundles (Fig 3A, white arrowheads). *H. miamia* possesses an external body wall muscle, and more internally, tissue Layer I, another muscle wall, and then tissue Layer II [38]. There is a relatively loose anterior condensation of e.g. GABAergic, dopaminergic, and peptidergic neurons in the anterior third of the animal in layer II, and various peripheral neurons are found throughout the animal in both layers (Fig 3B, [38]). In the young adult *H. miamia*, we observed high ASIC expression in cells throughout the anterior condensation (Fig 3B). Similar to *I. pulchra*, the ASIC signal is strongest near the dorsal commissure but, in contrast, also in scattered cells across the animal, including in the very periphery (Fig 3B, yellow arrowhead). The latter are present in inner and outer layers and are thus consistent with the dispersed, diverse neurons found in layers I and II of the animal. *C. macropyga* ASIC expression was high and broad. In the anterior, ASIC-expressing cells are clearly associated with the brain (Fig 3C', white arrowheads). Throughout the animal, including the very periphery, there is medium to high ASIC expression. While perhaps indicative of expression in locomotory ciliated cells covering the animal, this expression may be part of the extensive nerve plexus (Fig 3C''). In summary, *I. pulchra* shows localized, central ASIC expression whereas *C. macropyga* and *H. miamia* show both central and scattered, peripheral ASIC expression. Thus, ASIC is expressed in two distinct domains in Xenacoelomorpha: a central domain, and a peripheral domain, and ASICs are likely to have performed central, integrative and peripheral, sensory roles in early acoels.

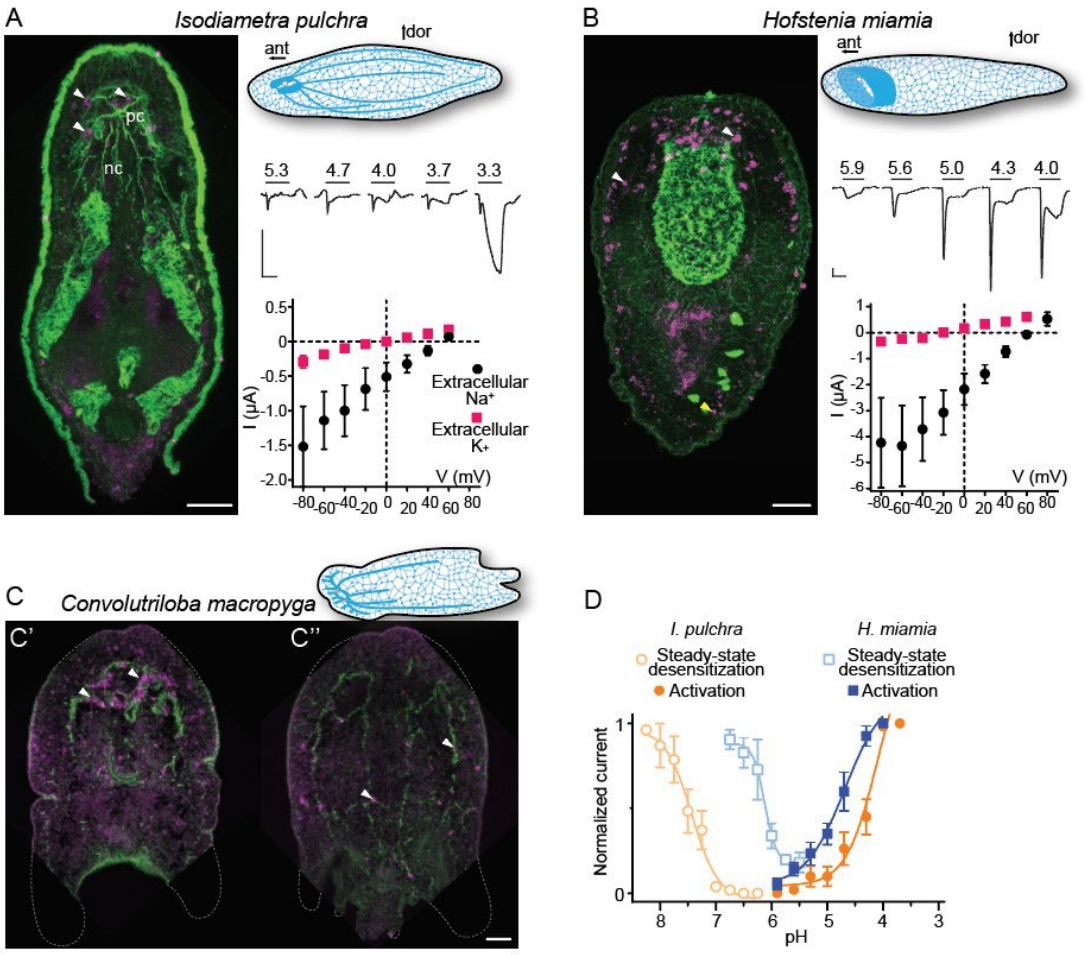

Fig 3. Expression and function of ASICs in Xenacoelomorpha. (A,B) Left: fluorescent confocal micrograph showing ASIC mRNA expression (magenta) and tyrosinated tubulin immunoreactivity (green), scale bar 40 µm. Upper right: cartoons illustrating morphology and nervous system (blue)

after [33]. ant, anterior; dor, dorsal; nb, neurite bundles; pc, posterior commissure. Mid-right: proton-gated currents in *Xenopus laevis* oocytes expressing xenacoelomorph ASICs (scale bars: x, 5 s; y, 0.5 µA). Lower right: Mean (± SEM) pH 4-gated current (I, µA) at different membrane potentials (V, mV) in the presence of 96 mM extracellular NaCl or KCl (n = 7-8). Reversal potential (V_{rev}) was read off these plots and the difference between $V_{rev,NaCl}$ and $V_{rev,KCl}$ was used to calculate relative ion permeability (P_{Na+}/P_{K+}, *Materials and Methods*). (C) ASIC mRNA expression (magenta) and tyrosinated tubulin immunoreactivity in *C. macropyga*. As *C. macropyga* is larger, images of slightly ventral (C') and dorsal (C") planes are shown. (D) Filled symbols: mean (± SEM) normalized current amplitude in response to increasing proton concentrations (activation, n = 6-10). Open symbols: mean (± SEM) normalized current amplitude in response to pH 4 following pre-incubation in decreasing pH (steady state desensitization, n = 4-6).

Xenacoelomorph ASICs mediate excitatory currents gated by high proton concentrations

When ASICs are exposed to drops in extracellular pH they typically show a transient depolarizing current (inward flow of Na^+ ions), rapidly followed by either desensitization—a non-ion-conducting state in the presence of agonist—or a smaller sustained current [39]. To test the function of xenacoelomorph ASICs, we injected the ASIC cRNAs into *Xenopus laevis* oocytes and measured membrane current in response to decreasing pH using two-electrode voltage clamp. At oocytes expressing *I. pulchra* ASIC, drops to pH 5.0 and lower rapidly activated a transient current (Fig 3A, mid- right). However, compared to other ASICs, responses to increased proton concentrations were relatively inconsistent at *I. pulchra* ASIC: although transient currents were never activated by pH higher than 5.6, the concentration dependence of the transient current between pH 5.3 and 4.0 was inconsistent, and a sustained current developed during prolonged proton application at pH ~4.0 in some cells and at pH ~3 in others (Fig 3A, mid-right). Thus, *I. pulchra* ASIC is indeed gated by protons, but with relatively low potency (pH for half-maximal activation of transient current (pH_{50}) = 4.0 ± 0.2). The *H. miamia* ASIC also formed proton-gated channels, with rapid transient currents followed by smaller sustained currents in response to drops to pH 5.6 through 4.0 (pH_{50} = 4.8 ± 0.1, Fig 3B,D). We observed no proton-gated currents in *Xenopus* oocytes injected with *C. macropyga* ASIC cRNA (n = 6), presumably due to low heterologous expression. Like vertebrate ASICs, *I. pulchra* and *H. miamia* ASICs showed decreased responses to activating pH (4.0) after preincubation in slightly decreased pH (Fig 3D, open symbols), indicating that steady-state desensitization is a broadly conserved phenomenon.

Most ASICs so far studied have a slight preference for sodium over potassium ions, with a relative sodium/potassium ion permeability (P_{Na+}/P_{K+}) of ~10, and thus activation of ASICs leads to depolarization and generation of action potentials in mice [40]. *I. pulchra* ASIC (P_{Na+}/P_{K+} = 8.3 ± 2.0) showed similar Na^+ selectivity to most ASICs (Fig 3A, lower right), whereas *H. miamia* Na^+ selectivity (P_{Na+}/P_{K+} = 36 ± 11; Fig 3B) is remarkably high compared to most ASICs and is more reminiscent of the high preference for sodium seen in ENaCs [41]. Thus, both in xenacoelomorphs, which belong to the putative, sister group to all other bilaterians, and in deuterostomes, such as rodents and humans, ASICs are excitatory receptors for protons that are expressed highly in both the central nervous system and in peripheral neurons.

ASICs are expressed in peripheral neurons and the digestive system in Spiralia

Excitatory proton-gated currents and broad neuronal expression of ASICs in xenacoelomorphs is reminiscent of vertebrate ASICs. However, whether the ancestral bilaterian ASIC had this role remains unclear, as the position of Xenacoelomorpha as sister taxon of all other bilaterians or as part of a group with hemichordates and echinoderms within Deuterostomia is debated [27-30]. We therefore turned to the third major lineage of bilaterians and investigated previously unidentified ASICs in Protostomia. We investigated the expression and function of ASICs in brachiopod, phoronid, and annelid larvae,

allowing us to study whole-animal gene expression in animals with typical spiralian features such as an anterior brain or apical organ and ventrolateral or peripherally extending nerve cords.

In the brachiopod *Terebratalia transversa*, ASIC was expressed most highly in cells at the lateral edge of the central neuropil in late larvae (Fig 4A). Confocal images suggest that these ASIC-expressing neurons project latero-anteriorly (Fig 4A, inset), suggesting an anterior sensory role, and these cells are slightly lateral/caudal to previously identified sensory neurons in the *T. transversa* apical organ [42], in close proximity to previously described cholinergic and peptidergic cells [33, 43]. In the phoronid *Phoronopsis harmeri*, ASIC was expressed in two principal domains. Regarding the nervous system, there was a clear signal in relatively few cells in the perimeter of the hood (Fig 4B, black arrowheads). This area is innervated by the peripheral nerve ring and controls swimming by ciliary beating [44, 45]. Whether the ASIC-positive cells have a role in chemosensing or controlling ciliary beating remains unclear. There was no ASIC expression in the more central parts of the nervous system, including both the apical organ, an anterior group of sensory neurons that gives way to the developing brain, and the main nerve ring that runs caudally from the apical organ through the trunk and innervates the tentacles [45-47]. The second domain, in which expression was even more prominent than that in the peripheral nervous system, was the digestive system. Here, expression was high in numerous cells around the digestive tract (comprising a stomach in the trunk and intestine in the pedicle at this stage), most noticeably just below the pharynx and around the lower half of the stomach (Fig 4B, orange arrowheads, [48]). We also detected such digestive system expression in the more distantly related spiralian, the annelid *Owenia fusiformis*. In dome-shaped *O. fusiformis* larvae 18-20 hours post fertilization (hpf), the young nervous system consists of a dorsal apical organ, several ventral prototroch (or ciliary band) neurons, and a small number of anterior and lateral neurons connecting these apical and peripheral structures [49, 50]. In 19 hpf *O. fusiformis*, we observed no ASIC expression in the young nervous system. Instead, ASIC was expressed most clearly in cells around the oesophagus, and, more broadly, in the midgut (Fig 4C). These results show that ASICs are expressed in the peripheral nervous system and/or epithelial cells in the digestive system of all spiralians tested.

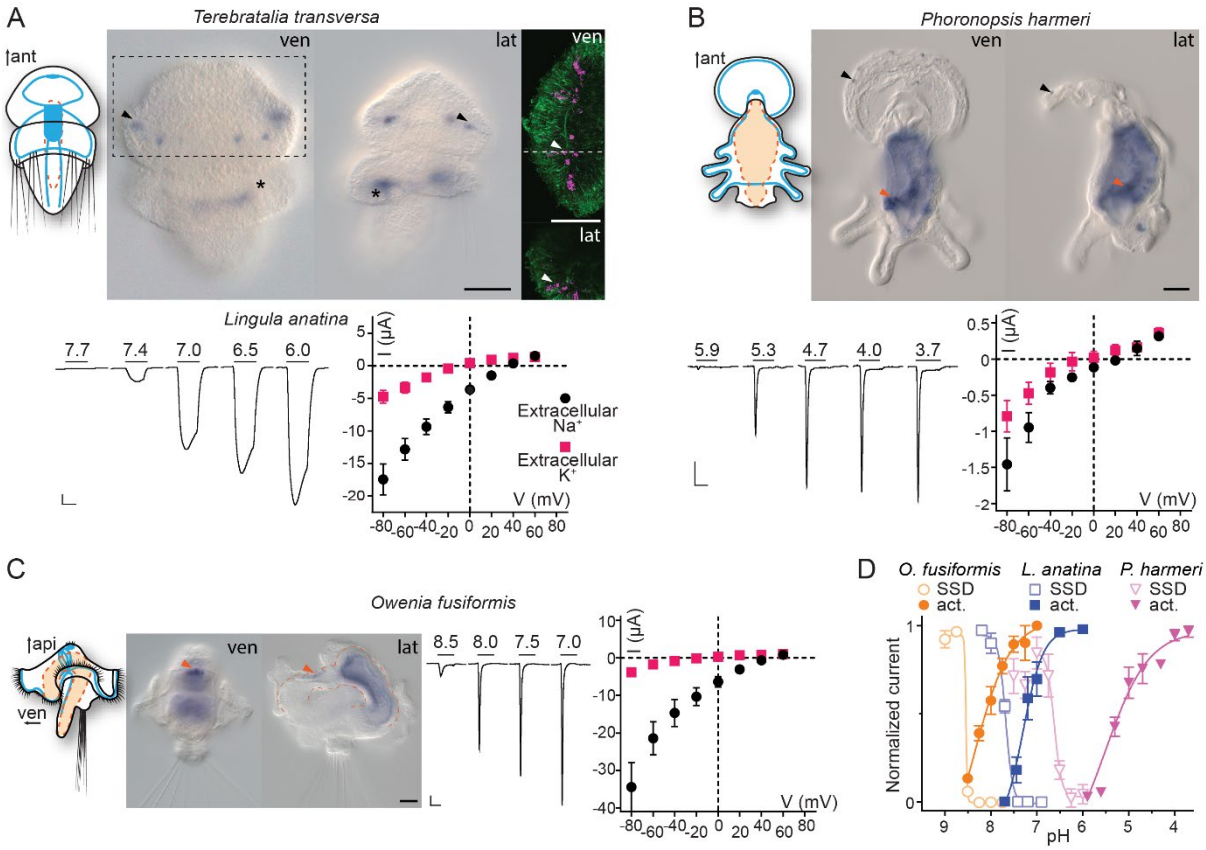

Fig 4. Expression and function of ASICs in Spiralia. (A,B) Upper: cartoons illustrating nervous system (blue) and digestive system (orange; Anlage only in *T. transversa*) after [50, 51] and ASIC mRNA expression (ant, anterior; api, apical; lat, lateral; ven, ventral; scale bar, 40 μm). Arrowheads, ASIC expression; asterisks, unspecific staining common in *T. transversa* [33]. Lower left: proton-gated currents in *Xenopus laevis* oocytes expressing indicated spiralian ASICs (scale bars: x, 5 s; y, 1 μA). Lower right: mean (± SEM) pH 6.5- (*L. anatina*) or 4- (*P. harmeri* ASIC) gated current (I, μA) at different membrane potentials (V, mV) in the presence of 96 mM extracellular NaCl or KCl (n = 5-8). Reversal potential (V_{rev}) was read off these plots and the difference between $V_{rev,NaCl}$ and $V_{rev,KCl}$ was used to calculate relative ion permeability (P_{Na+}/P_{K+}). (C) Left to right: Animal morphology, ASIC expression, proton-gated currents, and pH 6.0-gated current at different membrane potentials, as in (A,B) at *O. fusiformis* ASIC. (D) Filled symbols: mean (± SEM) normalized current amplitude in response to increasing proton concentrations (activation, "act.", n = 6-11). Open symbols: mean (± SEM) normalized current amplitude in response to pH 7 for *O. fusiformis*, 6.5 for *L. anatina*, and 4 for *P. harmeri* ASIC following pre-incubation in decreasing pH (steady state desensitization, n = 4-5).

Spiralian ASICs show a wide range of proton sensitivity and ion selectivity

We next tested the electrophysiological properties of spiralian ASICs by expressing them heterologously in *Xenopus* oocytes. We observed no proton-activated currents in *Xenopus* oocytes injected with *T. transversa* ASIC RNA (n = 10), and we cannot conclude if this is due to low heterologous expression or unknown function of this channel. However, we identified an ASIC transcript in another brachiopod, *Lingula anatina* [52], and observed functional expression of this channel. *L. anatina* ASIC was sensitive to relatively low proton concentrations, activated by pH in the range of 7.4 to 6.0 (Fig 4A, pH_{50} = 7.3 ± 0.2) and showed typical selectivity for sodium over potassium ions (Fig 4A, P_{Na+}/P_{K+} = 9.0 ± 1.7). The phoronid *P. harmeri* ASIC showed much lower proton sensitivity, with small currents in response to pH 5.3 and lower that rapidly desensitized in the continued presence of low pH (Fig 4B, pH_{50} = 5.1 ± 0.1) with almost no preference for sodium over potassium ions (Fig 4B, P_{Na+}/P_{K+} = 3.0 ± 0.9). We next tested the function of ASIC from the annelid *O. fusiformis*. This channel was also highly sensitive to low proton concentrations. When held at pH 7.5 and exposed

to lower pH, *O. fusiformis* ASIC showed very small current responses, but when held at pH 9.0 and exposed to small drops in pH, large inward currents were activated that rapidly desensitized (Fig 4C, pH_{50} = 8.1 ± 0.1). *O. fusiformis* ASIC also showed ion selectivity typical of most ASICs (Fig 4C, P_{Na+}/P_{K+} = 12.0 ± 0.3).

Spiralian ASICs seem to vary in apparent proton affinity and in ion selectivity among the lineages, from low proton sensitivity (pH ~5) and essentially non-selective cation currents in phoronid ASIC to high proton sensitivity (pH 7-8) and ~10-fold selective sodium permeability in brachiopod and annelid ASICs. All showed canonical steady-state desensitization, occurring in pH ranges higher than activating pH. Spiralian ASIC genes thus encode proton-gated cation channels, and ASICs are present in all major groups of bilaterians: Xenacoelomorpha, Protostomia, and Deuterostomia.

Hemichordate ASIC is expressed in peripheral cells and pharynx and mediates rapidly desensitizing excitatory currents in response to protons

Deuterostome ASIC expression and function have so far only been characterized in Olfactores (tunicates and vertebrates) [12, 23, 53], and relatively little is known about ASICs in the ambulacrarian lineage (echinoderms and hemichordates). Recent studies on neural development in sea urchin (*Lytechinus variegatus*) larvae showed that ASIC is expressed diffusely throughout the ciliary band [24]. This transcript (MH996684) is closely related to the Group B ASICs from echinoderms and hemichordates that showed proton-gated currents when expressed heterologously [12]. Here, we used the hemichordate *Schizocardium californicum* to characterize the combined expression and function of an ambulacrarian ASIC. *S. californicum* ASIC expression was visible in late larval stages when structures such as the nervous system and the ciliary bands become more intricate, like the sea urchin ASIC. The tornaria larva of *S. californicum* has two main ciliary bands: the circumoral band for feeding; and the telotroch, innervated by serotonergic neurites, for locomotion [54]. *S. californicum* ASIC expression was detected in both ciliary bands (Fig 5A, black arrowheads) as well as in the pharynx (Fig 5A, orange arrowhead), however, signal intensity was variable between specimens and sometimes difficult to detect in all domains. When heterologously expressed, *S. californicum* ASIC showed rapidly activating and desensitizing currents in response to extracellular acidification with proton sensitivity comparable to other hemichordate ASICs but lower than echinoderm ASICs (Fig 5B, pH_{50} = 5.3 ± 0.1) [12]. The *S. californicum* channel showed relatively weak ion selectivity, with P_{Na+}/P_{K+} values slightly above unity (2.9 ± 0.5; Fig 5D), similar to ion selectivity in previously described ambulacrarian ASICs [12]. *S. californicum* thus presents a functional ASIC that is expressed in the peripheral nervous system and the digestive system, and it appears that such peripheral expression of ASICs is a conserved feature of Deuterostomia, Protostomia, and Xenacoelomorpha.

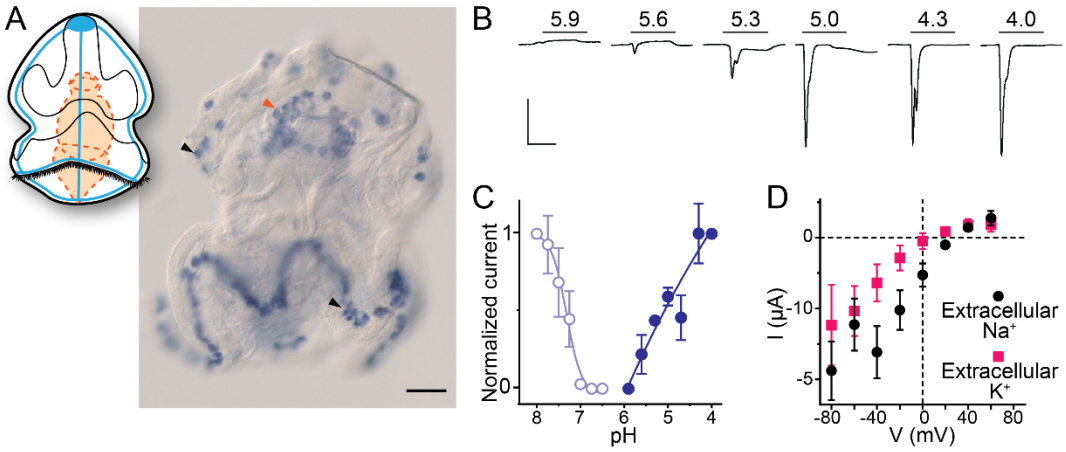

Fig 5. Expression and function of hemichordate ASIC. (A) Cartoon illustrating nervous system (blue) and digestive system (orange) in *Schizocardium californicum*, after [54], and colorimetric in situ hybridization showing *S. californicum* ASIC expression. Scale bar: 50 μm. (B) Proton-gated currents in *Xenopus laevis* oocytes expressing *S. californicum* ASIC. Scale bars: x, 5 s; y, 2 μA. (C) Filled symbols: mean (± SEM) normalized current amplitude in response to increasing proton concentrations (activation, "act.", n = 5). Open symbols: mean (± SEM) normalized current amplitude in response to pH 4 following pre-incubation in decreasing pH (steady state desensitization, n = 4).

Finally, we questioned if ASICs from Group A and Group B clades show characteristic functional differences. In terms of ion selectivity, Group B ASICs in deuterostomes show low sodium/potassium selectivity (P_{Na+}/P_{K+} between one and three), whereas Group B ASICs in protostomes and numerous Group A ASICs from deuterostomes and xenacoelomorphs have ~10-fold preference for sodium ions. In terms of apparent affinity for protons, large variability within Groups A and B is observed, with pH_{50} values for activation ranging from ~4 to ~8 in both groups. Thus, we see no convincing evidence of functional characteristics that distinguish Group A and Group B ASICs.

Discussion

The emergence of ASICs

Our results show that ASICs are present in Xenacoelomorpha and Protostomia in addition to Deuterostomia and are thus conserved in the three major groups of Bilateria. We also find, consistent with previous studies, that ASICs are absent from the other major lineages of Cnidaria, Placozoa, Porifera, and Ctenophora, despite the presence of other DEG/ENaC genes. This indicates that bona fide ASICs emerged in the lineage to the Bilateria, soon after the Cnidaria/Bilateria split ~800 Mya [55-57]. The closest relatives of ASICs within the DEG/ENaC tree include bile acid-gated channels (BASICs), certain peptide-gated channels (HyNaC), and a recently described leak channel (TadNaC6). BASICs are highly expressed in mammal intestines [58], HyNaCs are mostly expressed in the base of the tentacles near the mouth of the cnidarian *Hydra vulgaris* [11]; and TadNaC6 is expressed throughout the placozoan *Trichoplax adhaerans* [25]. Although none of these channels are activated by protons, the respective activity of BASICs and TadNaC6 is *inhibited* by increased proton concentrations ([25, 59]; S1 Fig). Although statistical support for the distinct ASIC clade is strong, we can unfortunately not resolve the precise relationships between HyNaC, BASIC, and ASIC clades, as branch support toward the base of the HyNaC+BASIC+ASIC group is relatively low (S1 Fig). Nonetheless, we think the most likely scenario is that the first ASIC emerged from a gene encoding another ligand-gated channel that was inhibited by protons. Golubovic et al. [60] have suggested that most DEG/ENaC channels, including ASICs, derive from a peptide-gated channel, noting that mammalian ASIC function is also modulated by cnidarian neuropeptides.

We infer that early bilaterians had two ASIC genes of similar proton-gated excitatory channel function, corresponding to Group A and Group B ASICs. Subsequently, and at different times, most descendants lost one of these (Fig 6). Acoels lost Group B ASIC and xenoturbellans lost Group A ASIC soon after this early split within the Xenacoelomorpha. In contrast, the first deuterostomes and, even more recently, the first chordates likely retained both ASICs, reflected in the continued presence of both in Cephalochordata (Fig 2). Subsequently, in Olfactores, Group B ASIC was lost and Group A ASIC underwent independent radiations, leading to e.g. ASIC1-ASIC4 paralogues in vertebrates [61], two Group A ASICs in tunicates [12], and multiple Group A ASICs in Cephalochordates (Fig 2).

Peripheral and central roles for ASICs

Although a broad division of the nervous system in numerous animals into central and peripheral is perhaps oversimplified [62], our results point toward ASIC expression in two distinct domains: the central nervous system, including brain and/or nerve cords; and in peripheral cells, in some cases

epithelia and in other cases peripheral neurons. This points to at least two functions of ASICs: a central signaling role, where ASICs mediate rapid excitatory signals between neurons in the brain [21]; and a peripheral sensory/modulatory role, where ASICs convert increased proton concentrations in the environment—extra-organismal or in the gut—into excitatory neuronal signals [63]. In Xenacoelomopha, we found central ASICs are suitably expressed to mediate signals between nerve cord neurons and the brain or between neurons within the brain, supported by high expression of synaptotagmin in the *I. pulchra* brain lobes and proximal nerve cords [33], where ASIC is expressed. This central role has been best characterized in the mouse brain, where presynaptic release of acidic glutamatergic vesicles leads to rapid increases in the concentration of both glutamate and protons in the synapse, activating postsynaptic glutamate receptors and ASICs to depolarize postsynaptic neurons [21, 22, 64]. High expression of zebrafish ASICs in the CNS suggests a similar role in synaptic communication in other vertebrates [61]. We observed central ASICs in only one of the three Spiralia tested, and these showed projections towards the very anterior of the animal, perhaps indicative of a less integrative and more sensory role. Thus, brain ASICs are common to Xenacoelomorpha and Deuterostomia and are less prevalent in Protostomia, and this central role is more commonly played by Group A ASICs than Group B ASICs (Fig 6).

The second and peripheral domain, observed in five of the six species of Xenacoelomorpha and Spiralia studied here, largely corresponds to the ciliation in the species. While xenacoelomorphs are completely covered with ciliated epithelial cells, in many other Bilateria the ciliation is restricted to ciliary bands or the ciliary ventral region, both used for locomotion. These ASICs are thus expressed in a location to sense external changes in pH and directly modulate ciliary movement via excitatory current or, via depolarization and synaptic release onto more central neurons, send the information centrally. Regarding the latter possibility, activation of ASICs by protons can generate action potentials in cultured mouse spinal neurons [40], but whether ASIC activation could trigger synaptic release from such sensory cells, or whether xenacoelomorph ciliary cells are capable of pre-synaptic signaling like chordate sensory cells [65], is unknown. Conversely, if these ASICs are expressed on the proximal side of the epithelial cells, their role may be modulation of ciliary function in response to efferent modulatory signals. Although activation of postsynaptic ASICs has so far been linked to only glutamatergic and GABAergic synapses [21, 66] and innervation of ciliary cells appears serotonergic in Spiralia [44], monoaminergic vesicles are also acidic and could thus foreseeably release protons to activate ASICs here [67].

We were surprised to see expression of ASIC predominantly in the digestive system of the spiralians *O. fusiformis* and *P. harmeri*. In mammals, chemosensors such as ASIC and transient receptor potential channels (e.g. TRPV1) are expressed in sensory neurons innervating the gastrointestinal tract [17], but oesophageal, intestinal, and lung epithelial cells also express ASICs, potentially contributing to acid-induced secretions, transport, and inflammation [68-70]. The gastrointestinal expression of ASICs may reflect a chemosensory role, like that mediated by ASICs in neurons innervating the lungs and skin of mammals [71, 72]. Similar functions are suggested by ASIC expression in the peripheral nervous system of other chordates and Ambulacraria ([24, 73], Fig 5). Again, we can't exclude the possibility that these peripheral ASICs are modulating ciliary function, either directly via acid-induced activation or indirectly, via efferent signals from central neurons. Nonetheless, these expression patterns seem to suggest that ASICs play a sensory role in the peripheral nervous system of Deuterostomia, Protostomia, and Xenacoelomorpha via expression in (basi-)epithelial or peripheral nervous system neurons, indicating that such a role was probably present in the ancestral bilaterian. Consistent with the early appearance of this role, it is played by both Group A and Group B ASICs, which both emerged in early Bilateria. Subsequently, ASICs - particularly Group A - were likely deployed to the other, more central role for inter-neuronal communication in lineages such as Acoela and Chordata.

Loss of ASICs

The conservation and high expression of ASICs in bilaterians begs the questions as to why they were lost in certain lineages. The reason for the loss of ASICs in selected Spiralia, such as molluscs and platyhelminthes is unclear, especially when one considers that numerous molluscs are susceptible to the tide and thus vast fluctuations in pH. Presumably, gene radiations that increased sensory ion channel or transporter diversity in such animals have compensated for the loss of ASICs [74-78], and indeed, certain members of other channel families are capable of mediating excitation (or inhibition) in response to decreased pH [3]. Perhaps most noticeable, however, is the absence of ASICs in Ecdysozoa, a broad lineage including pan-arthropods, nematodes, and priapulids, each of which we considered in our phylogenetic analysis. Ecdysozoa split from Spiralia 600-800 Mya [55-57], adopting a chitinous cuticle utilizing rigid locomotory structures and requiring periodic molting for growth [79, 80]. Concomitantly, Ecdysozoa lost the ectodermal, motile ciliated cells inherited from the last common ancestor of Cnidaria and Bilateria that mediate locomotory, feeding, secretory, and sensory functions in most other bilaterians [81, 82]. The correlation between loss of ASICs and loss of motile ciliated cells, together with the conservation of other ciliated and sensory cells in Ecdysozoa, indicates that the role of ASICs in early Protostomia was primarily associated with ectodermal ciliated cells rather than more central sensory cells associated with e.g. mouth, eyes, and antennae. This, together with the presence of ASICs in the periphery of Xenacoelomorpha and Deuterostomia, suggests that the role of the earliest ASIC was likely local conversion of external chemical stimuli into modulation of locomotion, conversion of central signals into modulation of locomotion, or both. Indeed, motile ciliated epithelia in human lungs are modulated by both external and central stimuli [83], although the precise contribution of ASICs in these cells is unclear [69].

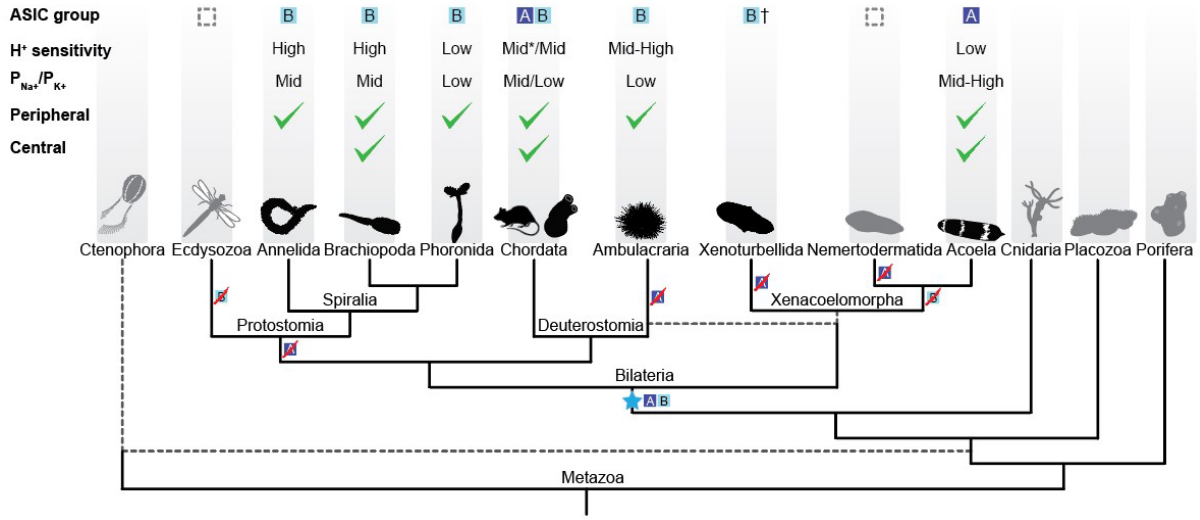

Figure 6. Evolutionary history of ASIC function in Metazoa. Upper half of diagram indicates characteristic properties of ASIC in different lineages: DEG/ENaC gene tree position ("ASIC group A or B"); proton (H^+) sensitivity; relative ion permeability ("P_{Na+}/P_{K+}"); native expression pattern ("Peripheral", ciliary or gastrointestinal epithelia and/or peripheral neurons; "Central", brain and/or nerve cords). Lower half shows phylogenetic relationships of the different animal phyla studied here. Blue star, putative emergence of ASICs in the last common ancestor of all bilaterians after Cnidaria/Bilateria split. For H^+ sensitivity, "low", "mid", and "high" correspond to pH_{50} <5.3, 5.3-7, and >7, respectively. *, a minority of characterized chordate ASICs have low H^+ sensitivity ([41, 61]). For relative ion permeability, "low", "mid", and "high" correspond to P_{Na+}/P_{K+} ≤3, 3-15, and >15, respectively. †, channel function not experimentally tested.

Outlook

We acknowledge that future experiments might benefit from greater genomic resources from non-bilaterian animals, but our comprehensive survey of DEG/ENaC genes from Ctenophora, Porifera, Placozoa, and Cnidaria finds no ASICs in those lineages. Our study suggests that ASICs emerged in an early bilaterian, most likely in peripheral neurons or epithelia, and were gradually adopted into the central nervous system of certain complex animals. This offers a unique insight into the role of LGICs in early bilaterian evolution. Functional characterization of diverse ASICs shows a considerable breadth of pH sensitivity and ion selectivity throughout the family, offering new tools for probing the biophysical mechanisms of function. The combined use of gene expression and function is thus a useful tool in understanding protein evolution and function.

Materials and Methods

Survey and phylogenetic analysis

Mouse ASIC1a was used as a query in tBLASTn searches of DEG/ENaC genes in xenacoelomorphs (*Convolutriloba macropyga, Childia submaculatum, Hofstenia miamia, Isodiametra pulchra, Xenoturbella bocki, Xenoturbella profunda, Nemertoderma westbladi,* and *Meara stichopi* from transcriptomes published in [84]), spiralians (*Spadella spp., Dimorphilus gyrociliatus, Epiphanes senta, Lepidodermella squamata, Lineus longissimus, Lineus ruber, Membranipora membranacea, Novocrania anomala, Owenia fusiformis, Phoronopsis harmeri, Prostheceraeus vittatus,* and *Terebratalia transversa* from our transcriptomes in preparation; *Acanthopleura granulata, Crassostrea gigas*, and *Brachionus plicatilis* from NCBI; *Lingula anatina* and *Notospermus geniculatus* from OIST; and *Schmidtea mediterranea* from SmedGD), ecdysozoans (*Halicryptus spinulosus, Priapulus caudatus, Pontonema vulgare* from our transcriptomes; *Drosophila melanogaster, Daphnia pulex, Centruroides sculpturatus* and *Caenorhabditis elegans* from NCBI) and a hemichordate (*Schizocardium californicum,* our transcriptome). Other DEG/ENaC genes were retrieved via BlastP at public databases NCBI, Compagen, JGI, OIST, OikoBase, Aniseed, or UniProt targeting cnidarians (hexacorallian *Nematostella vectensis*, octacorallian *Dendronephthya gigantea*, scyphozoan *Aurelia aurita*, hydrozoan *Hydra vulgaris*), poriferan (*Amphimedon queenslandica*), the placazoan *Trichoplax adhaerens*, ctenophores (cydippid *Pleurobrachia bachei* and lobate *Mnemiopsis leidyi*), and deuterostomes (chordates *Rattus norvegicus, Ciona robusta, Oikopleura dioica* and *Branchiostoma belcheri*; hemichordate *Ptychodera flava*; and echinoderm *Acanthaster planci*). Amino acid sequences were aligned using MAFFT [85], variable N- and C-termini were removed and highly similar sequences were not considered (S1 Text), and homologies were assigned by phylogenetic tree analyses based on Maximum Likelihood (ML) inferences calculated with PhyML v3.0 [86]. Robustness of tree topologies was assessed under automatic model selection based on Akaike Information Criteria. Due to computational load limitation of bootstrap performance, branch support was inferred by fast likelihood-based methods aLRT SH-like and aBayes [87].

Animal collections and fixations

Stable cultures of acoels were maintained in the laboratory. *Convolutriloba macropyga* [88] were reared in a tropical aquarium system with salinity 34+/-1 ppt at a constant temperature of 25 °C. The aquariums were illuminated (Pacific LED lamp WT470C LED64S/840 PSU WB L1600, Philips) on a day/night cycle of 12/12 hours. The worms were fed with freshly hatched brine shrimp *Artemia* twice per week. *Isodiametra pulchra* [89] were cultured as described by [90], and *Hofstenia miamia* [91] as described by [92]. For the remaining species, adult gravid animals were collected from Bodega Bay, California, USA (*Phoronopsis harmeri* [93]), San Juan Island, Washington, USA (*Terebratalia transversa* [94]), Station Biologique de Roscoff, France (*Owenia fusiformis* [95]), and Kanangra Boyd National Park and Morro Bay State Park, California, USA (*Schizocardium californicum* [96]). Animals were spawned and

larvae obtained as described in [97-100]. Adult and larval specimens were starved for 2 - 7 days prior to fixation. Samples were relaxed in 7.4% magnesium chloride and fixed in 4% paraformaldehyde in culture medium for 1 hour at room temperature and washed several times in 0.1% Tween 20 phosphate buffered saline (PBS), dehydrated through a graded series of methanol, and stored in pure methanol or ethanol at −20 °C.

Cloning

The full-length coding sequences of identified ASIC genes were amplified from cDNA of *C. macropyga*, *I. pulchra*, *H. miamia*, *P. harmeri*, *O. fusiformis*, *T. transversa*, and *S. californicum* by PCR using gene-specific primers. PCR products were purified and cloned into a pGEM-T Easy vector (Promega, A1360) according to the manufacturer's instructions and the identity of inserts confirmed by sequencing. Riboprobes were synthesized with Ambion Megascript T7 (AM1334) and SP6 (AM1330) kit following manufacturer's instruction for subsequent in situ hybridization.

Immunohistochemistry and situ hybridization

Single whole-mount colorimetric and fluorescent in situ hybridization was performed following an established protocol [31] with probe concentration of 0.1 ng/µl (*I. pulchra*) or 1 ng/µl (the remaining species) and hybridization temperature of 67 °C. Proteinase K treatment time was adjusted for each species and ranged from 2 minutes (*P. harmeri, O. fusiformis, S. californicum*) to 10 minutes (*T. transversa).* Post-hybridization low salt washes were performed with 0.05x saline sodium citrate (SSC; *H. miamia*) or 0.2x SSC (the remaining species). Fluorescent in situ hybridization was visualized with TSA Cy3 kit (PerkinElmer, NEL752001KT). Samples were mounted in 70% glycerol or subjected to immunohistochemistry for visualization of neural structures: samples were permeabilized in 0,2 % Triton-x in PBS (PTx) and blocked in 1% bovine serum albumin in PTx (PBT) and incubated with antibodies against tyrosinated tubulin (Sigma, T9028) at a concentration of 1:250 in PTx with 5% normal goat serum, and incubated for 16-18 hours at 4 °C. After several washes in PBT the samples were incubated with secondary goat anti-mouse antibodies conjugated with AlexaFluor 488 (Life Technologies), at a concentration 1:200 in PTx with 5% normal goat serum for 16-18 hours at 4 °C, and samples washed extensively before mounting in 70 % glycerol and imaging. Nuclei were stained with DAPI (Molecular Probes).

Imaging

Representative specimens from colorimetric in situ hybridization experiments were imaged with a Zeiss Axiocam 503 color connected to a Zeiss Axioscope 5 using bright-field Nomarski optics. Fluorescently labelled samples were scanned in an Olympus FV3000 confocal laser-scanning microscope. Colorimetric in situ's stained with antibodies were scanned in a Leica SP5 confocal laser-scanning microscope using reflection microscopy protocol as described by [101]. Images were analyzed with Imaris 9.8.0 and Photoshop CS6 (Adobe), and figure plates were assembled with Illustrator CC. Brightness/contrast and color balance adjustments were applied to the whole image, not parts.

Electrophysiological recordings and data analysis

For expression in *Xenopus laevis* oocytes and electrophysiological experiments, coding sequences were mutated synonymously to remove internal restriction sites if necessary and subcloned into SalI and XbaI sites of a modified pSP64poly(A) vector (ProMega), containing 5' SP6 sequence, 5′- and 3′-UTR sequences of the *X. laevis* β-globin gene, and a C-terminal Myc tag, with an EcoRI restriction site after the poly(A) tail (S2 Text). *Lingula anatina* ASIC (g20471.t1 from *Lingula anatina* Ver 2.0, OIST Marine Genomics Unit), synonymously mutated to remove internal restriction sites and including a C-terminal myc tag before the stop codon, was commercially synthesized and subcloned (Genscript) into

HindIII and BamHI sites of pSP64poly(A) (S2 Text). Plasmids were linearized with EcoRI, and cRNA was synthesized in vitro with SP6 Polymerase (mMessage mMachine kit, Ambion). Stage V/VI *X. laevis* oocytes, purchased from Ecocyte Bioscience (Dortmund, Germany), were injected with 3-90 ng cRNA. After injection, oocytes were incubated for one to three days at 19°C in 50% Leibowitz medium (Merck) supplemented with 0.25 mg/ml gentamicin, 1 mM L-glutamine, and 15 mM HEPES (pH 7.6). Whole cell currents were recorded from oocytes by two-electrode voltage clamp using an OC-725C amplifier (Warner Instruments) and an LIH 8+8 digitizer with Patchmaster software (HEKA), acquired at 1 kHz and filtered at 200 Hz. Currents were also analyzed in pClamp v10.7 software (Molecular Devices) and additionally filtered at 1 Hz for display in figures. Oocytes were clamped at -60 mV, unless otherwise indicated, and continuously perfused with a bath solution containing (in mM): 96 NaCl, 2 KCl, 1.8 $CaCl_2$, 1 $MgCl_2$, and 5 HEPES (for pH > 6.0) or 5 MES (for pH ≤ 6.0). pH was adjusted with NaOH, HCl, or KOH, as appropriate. In most experiments, activating/desensitizing pH was applied to oocytes in between resting periods (at pH 7.5 for most ASICS, at pH 9.0, 8.6, and 8.0 for *O. fusiformis, L. anatina S. californicum* ASICs, respectively, unless otherwise indicated) of at least 30 s. After retrieving current amplitude from pClamp, all data analyses were performed in Prism v9 (GraphPad Software). In concentration-response graphs, currents are normalized to maximum proton-gated current. For ion selectivity experiments, IV relationships were measured in regular bath solution and that in which extracellular NaCl was replaced with KCl. IV relationships were obtained by activating the channels at different membrane potentials from -80 to 60 mV, with 20 mV increments, unless otherwise indicated. Reversal potentials ($V_{rev,Na+}$ and $V_{rev,K+}$) were taken from the intersection of the IV curve with the voltage axis. These values were used to calculate relative permeability P_{Na+}/P_{K+} with the Goldman-Hodgkin-Katz equation, $P_{Na+}/P_{K+} = \exp(F(V_{rev,Na+} - V_{rev,K+})/RT)$, where F = Faraday constant, R = gas constant, and T = 293 K. Standard chemicals were purchased from Merck. Specialist chemicals (S1 Fig) were purchased from Santa Cruz Biotechnology (item sc-222407, sodium ursodeoxycholic acid, ≥98% purity) or synthesized by Genscript ((pyroE)WLGGRFamide, ≥97% purity – "Hydra RFamide I" from [11]).

Acknowledgements

We thank Chris Lowe (Stanford University) for *Phoronopsis harmeri* and *Schizocardium californicum* samples.

References

1. Arendt D. Elementary nervous systems. Philosophical transactions of the Royal Society of London Series B, Biological sciences. 2021;376(1821):20200347. Epub 2021/02/09. doi: 10.1098/rstb.2020.0347. PubMed PMID: 33550948; PubMed Central PMCID: PMCPMC7935009.
2. Liebeskind BJ, Hillis DM, Zakon HH, Hofmann HA. Complex Homology and the Evolution of Nervous Systems. Trends in ecology & evolution. 2016;31(2):127-35. doi: 10.1016/j.tree.2015.12.005. PubMed PMID: 26746806; PubMed Central PMCID: PMC4765321.
3. Pattison LA, Callejo G, St John Smith E. Evolution of acid nociception: ion channels and receptors for detecting acid. Philosophical transactions of the Royal Society of London Series B, Biological sciences. 2019;374(1785):20190291. Epub 2019/09/24. doi: 10.1098/rstb.2019.0291. PubMed PMID: 31544616; PubMed Central PMCID: PMCPMC6790391.
4. Smart TG, Paoletti P. Synaptic neurotransmitter-gated receptors. Cold Spring Harbor perspectives in biology. 2012;4(3). doi: 10.1101/cshperspect.a009662. PubMed PMID: 22233560; PubMed Central PMCID: PMC3282413.
5. Chen GQ, Cui C, Mayer ML, Gouaux E. Functional characterization of a potassium-selective prokaryotic glutamate receptor. Nature. 1999;402(6763):817-21. Epub 2000/01/05. doi: 10.1038/45568. PubMed PMID: 10617203.
6. Chiu J, DeSalle R, Lam HM, Meisel L, Coruzzi G. Molecular evolution of glutamate receptors: a primitive signaling mechanism that existed before plants and animals diverged. Molecular

biology and evolution. 1999;16(6):826-38. Epub 1999/06/16. doi: 10.1093/oxfordjournals.molbev.a026167. PubMed PMID: 10368960.
7. Tasneem A, Iyer LM, Jakobsson E, Aravind L. Identification of the prokaryotic ligand-gated ion channels and their implications for the mechanisms and origins of animal Cys-loop ion channels. Genome Biol. 2005;6(1):R4. Epub 2005/01/12. doi: 10.1186/gb-2004-6-1-r4. PubMed PMID: 15642096; PubMed Central PMCID: PMCPMC549065.
8. Moroz LL, Kocot KM, Citarella MR, Dosung S, Norekian TP, Povolotskaya IS, et al. The ctenophore genome and the evolutionary origins of neural systems. Nature. 2014;510(7503):109-14. doi: 10.1038/nature13400. PubMed PMID: 24847885; PubMed Central PMCID: PMC4337882.
9. Liebeskind BJ, Hillis DM, Zakon HH. Convergence of ion channel genome content in early animal evolution. Proc Natl Acad Sci U S A. 2015;112(8):E846-51. doi: 10.1073/pnas.1501195112. PubMed PMID: 25675537; PubMed Central PMCID: PMC4345596.
10. Heger P, Zheng W, Rottmann A, Panfilio KA, Wiehe T. The genetic factors of bilaterian evolution. eLife. 2020;9:e45530. doi: 10.7554/eLife.45530.
11. Assmann M, Kuhn A, Durrnagel S, Holstein TW, Grunder S. The comprehensive analysis of DEG/ENaC subunits in Hydra reveals a large variety of peptide-gated channels, potentially involved in neuromuscular transmission. BMC Biol. 2014;12:84. doi: 10.1186/s12915-014-0084-2. PubMed PMID: 25312679; PubMed Central PMCID: PMCPMC4212090.
12. Lynagh T, Mikhaleva Y, Colding JM, Glover JC, Pless SA. Acid-sensing ion channels emerged over 600 Mya and are conserved throughout the deuterostomes. Proc Natl Acad Sci U S A. 2018;115(33):8430-5. Epub 2018/08/01. doi: 10.1073/pnas.1806614115. PubMed PMID: 30061402; PubMed Central PMCID: PMCPMC6099870.
13. Matthews BJ, Younger MA, Vosshall LB. The ion channel ppk301 controls freshwater egg-laying in the mosquito Aedes aegypti. eLife. 2019;8. Epub 2019/05/22. doi: 10.7554/eLife.43963. PubMed PMID: 31112133; PubMed Central PMCID: PMCPMC6597239.
14. Ng R, Salem SS, Wu S-T, Wu M, Lin H-H, Shepherd AK, et al. Amplification of Drosophila Olfactory Responses by a DEG/ENaC Channel. Neuron. 2019;104(5):947-59.e5. doi: https://doi.org/10.1016/j.neuron.2019.08.041.
15. Tavernarakis N, Shreffler W, Wang S, Driscoll M. unc-8, a DEG/ENaC Family Member, Encodes a Subunit of a Candidate Mechanically Gated Channel That Modulates C. elegans Locomotion. Neuron. 1997;18(1):107-19. doi: https://doi.org/10.1016/S0896-6273(01)80050-7.
16. Deval E, Lingueglia E. Acid-Sensing Ion Channels and nociception in the peripheral and central nervous systems. Neuropharmacology. 2015;94:49-57. doi: 10.1016/j.neuropharm.2015.02.009. PubMed PMID: 25724084.
17. Holzer P. Acid-sensing ion channels in gastrointestinal function. Neuropharmacology. 2015;94:72-9. Epub 2015/01/15. doi: 10.1016/j.neuropharm.2014.12.009. PubMed PMID: 25582294; PubMed Central PMCID: PMCPMC4458375.
18. Ikeuchi M, Kolker SJ, Burnes LA, Walder RY, Sluka KA. Role of ASIC3 in the primary and secondary hyperalgesia produced by joint inflammation in mice. Pain. 2008;137(3):662-9. Epub 2008/03/18. doi: 10.1016/j.pain.2008.01.020. PubMed PMID: 18343037; PubMed Central PMCID: PMCPMC2756650.
19. Jones NG, Slater R, Cadiou H, McNaughton P, McMahon SB. Acid-induced pain and its modulation in humans. The Journal of neuroscience : the official journal of the Society for Neuroscience. 2004;24(48):10974-9. doi: 10.1523/JNEUROSCI.2619-04.2004. PubMed PMID: 15574747.
20. Price MP, McIlwrath SL, Xie J, Cheng C, Qiao J, Tarr DE, et al. The DRASIC cation channel contributes to the detection of cutaneous touch and acid stimuli in mice. Neuron. 2001;32(6):1071-83. PubMed PMID: 11754838.
21. Du J, Reznikov LR, Price MP, Zha XM, Lu Y, Moninger TO, et al. Protons are a neurotransmitter that regulates synaptic plasticity in the lateral amygdala. Proc Natl Acad Sci U S A. 2014;111(24):8961-6. doi: 10.1073/pnas.1407018111. PubMed PMID: 24889629; PubMed Central PMCID: PMCPMC4066526.
22. Gonzalez-Inchauspe C, Urbano FJ, Di Guilmi MN, Uchitel OD. Acid-Sensing Ion Channels Activated by Evoked Released Protons Modulate Synaptic Transmission at the Mouse Calyx of Held Synapse. The Journal of neuroscience : the official journal of the Society for Neuroscience.

2017;37(10):2589-99. Epub 2017/02/06. doi: 10.1523/JNEUROSCI.2566-16.2017. PubMed PMID: 28159907; PubMed Central PMCID: PMCPMC6596635.
23. Coric T, Passamaneck YJ, Zhang P, Di Gregorio A, Canessa CM. Simple chordates exhibit a proton-independent function of acid-sensing ion channels. FASEB journal : official publication of the Federation of American Societies for Experimental Biology. 2008;22(6):1914-23. doi: 10.1096/fj.07-100313. PubMed PMID: 18211956.
24. Slota LA, Miranda E, Peskin B, McClay DR. Developmental origin of peripheral ciliary band neurons in the sea urchin embryo. Dev Biol. 2020;459(2):72-8. Epub 2019/12/28. doi: 10.1016/j.ydbio.2019.12.011. PubMed PMID: 31881199; PubMed Central PMCID: PMCPMC7080585.
25. Elkhatib W, Smith CL, Senatore A. A Na+ leak channel cloned from Trichoplax adhaerens extends extracellular pH and Ca2+ sensing for the DEG/ENaC family close to the base of Metazoa. Journal of Biological Chemistry. 2019;294(44):16320-36. doi: https://doi.org/10.1074/jbc.RA119.010542.
26. Foster VS, Rash LD, King GF, Rank MM. Acid-Sensing Ion Channels: Expression and Function in Resident and Infiltrating Immune Cells in the Central Nervous System. Frontiers in Cellular Neuroscience. 2021;15(376). doi: 10.3389/fncel.2021.738043.
27. Cannon JT, Vellutini BC, Smith J, 3rd, Ronquist F, Jondelius U, Hejnol A. Xenacoelomorpha is the sister group to Nephrozoa. Nature. 2016;530(7588):89-93. doi: 10.1038/nature16520. PubMed PMID: 26842059.
28. Kapli P, Natsidis P, Leite DJ, Fursman M, Jeffrie N, Rahman IA, et al. Lack of support for Deuterostomia prompts reinterpretation of the first Bilateria. Sci Adv. 2021;7(12). Epub 2021/03/21. doi: 10.1126/sciadv.abe2741. PubMed PMID: 33741592; PubMed Central PMCID: PMCPMC7978419.
29. Laumer CE, Fernandez R, Lemer S, Combosch D, Kocot KM, Riesgo A, et al. Revisiting metazoan phylogeny with genomic sampling of all phyla. Proc Biol Sci. 2019;286(1906):20190831. Epub 2019/07/11. doi: 10.1098/rspb.2019.0831. PubMed PMID: 31288696; PubMed Central PMCID: PMCPMC6650721.
30. Philippe H, Poustka AJ, Chiodin M, Hoff KJ, Dessimoz C, Tomiczek B, et al. Mitigating Anticipated Effects of Systematic Errors Supports Sister-Group Relationship between Xenacoelomorpha and Ambulacraria. Current Biology. 2019;29(11):1818-26.e6. doi: https://doi.org/10.1016/j.cub.2019.04.009.
31. Hejnol A, Pang K. Xenacoelomorpha's significance for understanding bilaterian evolution. Current opinion in genetics & development. 2016;39:48-54. doi: https://doi.org/10.1016/j.gde.2016.05.019.
32. Achatz JG, Martinez P. The nervous system of Isodiametra pulchra (Acoela) with a discussion on the neuroanatomy of the Xenacoelomorpha and its evolutionary implications. Front Zool. 2012;9(1):27. Epub 2012/10/18. doi: 10.1186/1742-9994-9-27. PubMed PMID: 23072457; PubMed Central PMCID: PMCPMC3488495.
33. Martín-Durán JM, Pang K, Børve A, Lê HS, Furu A, Cannon JT, et al. Convergent evolution of bilaterian nerve cords. Nature. 2018;553(7686):45-50. doi: 10.1038/nature25030.
34. Sikes JM, Bely AE. Radical modification of the A–P axis and the evolution of asexual reproduction in Convolutriloba acoels. Evolution & Development. 2008;10(5):619-31. doi: https://doi.org/10.1111/j.1525-142X.2008.00276.x.
35. Haszprunar G. Review of data for a morphological look on Xenacoelomorpha (Bilateria incertae sedis). Organisms Diversity & Evolution. 2016;16(2):363-89. doi: 10.1007/s13127-015-0249-z.
36. Martin GG. Ciliary gliding in lower invertebrates. Zoomorphologie. 1978;91(3):249-61. doi: 10.1007/BF00999814.
37. Raikova OI, Meyer-Wachsmuth I, Jondelius U. The plastic nervous system of Nemertodermatida. Organisms Diversity & Evolution. 2016;16(1):85-104. doi: 10.1007/s13127-015-0248-0.
38. Hulett RE, Potter D, Srivastava M. Neural architecture and regeneration in the acoel Hofstenia miamia. Proc Biol Sci. 2020;287(1931):20201198. Epub 2020/07/23. doi: 10.1098/rspb.2020.1198. PubMed PMID: 32693729; PubMed Central PMCID: PMCPMC7423668.

39. Krishtal O. Receptor for protons: First observations on Acid Sensing Ion Channels. Neuropharmacology. 2015;94:4-8. doi: 10.1016/j.neuropharm.2014.12.014. PubMed PMID: 25582296.
40. Gruol DL, Barker JL, Huang LY, MacDonald JF, Smith TG, Jr. Hydrogen ions have multiple effects on the excitability of cultured mammalian neurons. Brain research. 1980;183(1):247-52. Epub 1980/02/03. doi: 10.1016/0006-8993(80)90138-9. PubMed PMID: 7357408.
41. Grunder S, Pusch M. Biophysical properties of acid-sensing ion channels (ASICs). Neuropharmacology. 2015;94:9-18. doi: 10.1016/j.neuropharm.2014.12.016. PubMed PMID: 25585135.
42. Santagata S, Resh C, Hejnol A, Martindale MQ, Passamaneck YJ. Development of the larval anterior neurogenic domains of Terebratalia transversa (Brachiopoda) provides insights into the diversification of larval apical organs and the spiralian nervous system. EvoDevo. 2012;3(1):3. doi: 10.1186/2041-9139-3-3.
43. Thiel D, Bauknecht P, Jekely G, Hejnol A. An ancient FMRFamide-related peptide-receptor pair induces defence behaviour in a brachiopod larva. Open Biol. 2017;7(8). Epub 2017/08/25. doi: 10.1098/rsob.170136. PubMed PMID: 28835571; PubMed Central PMCID: PMCPMC5577450.
44. Marinkovic M, Berger J, Jekely G. Neuronal coordination of motile cilia in locomotion and feeding. Philosophical transactions of the Royal Society of London Series B, Biological sciences. 2020;375(1792):20190165. Epub 2019/12/31. doi: 10.1098/rstb.2019.0165. PubMed PMID: 31884921; PubMed Central PMCID: PMCPMC7017327.
45. Temereva EN, Tsitrin EB. Development and organization of the larval nervous system in Phoronopsis harmeri: new insights into phoronid phylogeny. Frontiers in Zoology. 2014;11(1):3. doi: 10.1186/1742-9994-11-3.
46. Nielsen C. Larval nervous systems: true larval and precocious adult. Journal of Experimental Biology. 2015;218(4):629-36. doi: 10.1242/jeb.109603.
47. Temereva EN, Tsitrin EB. Organization and metamorphic remodeling of the nervous system in juveniles of Phoronopsis harmeri(Phoronida): insights into evolution of the bilaterian nervous system. Frontiers in Zoology. 2014;11(1):35. doi: 10.1186/1742-9994-11-35.
48. Andrikou C, Passamaneck YJ, Lowe CJ, Martindale MQ, Hejnol A. Molecular patterning during the development of Phoronopsis harmeri reveals similarities to rhynchonelliform brachiopods. EvoDevo. 2019;10(1):33. doi: 10.1186/s13227-019-0146-1.
49. Carrillo-Baltodano AM, Seudre O, Guynes K, Martín-Durán JM. Early embryogenesis and organogenesis in the annelid Owenia fusiformis. EvoDevo. 2021;12(1):5. doi: 10.1186/s13227-021-00176-z.
50. Helm C, Vöcking O, Kourtesis I, Hausen H. Owenia fusiformis – a basally branching annelid suitable for studying ancestral features of annelid neural development. BMC Evolutionary Biology. 2016;16(1):129. doi: 10.1186/s12862-016-0690-4.
51. Gąsiorowski L, Andrikou C, Janssen R, Bump P, Budd GE, Lowe CJ, et al. Molecular evidence for a single origin of ultrafiltration-based excretory organs. Current Biology. 2021;31(16):3629-38.e2. doi: https://doi.org/10.1016/j.cub.2021.05.057.
52. Luo Y-J, Takeuchi T, Koyanagi R, Yamada L, Kanda M, Khalturina M, et al. The Lingula genome provides insights into brachiopod evolution and the origin of phosphate biomineralization. Nature Communications. 2015;6(1):8301. doi: 10.1038/ncomms9301.
53. Kellenberger S, Schild L. International Union of Basic and Clinical Pharmacology. XCI. structure, function, and pharmacology of acid-sensing ion channels and the epithelial Na+ channel. Pharmacol Rev. 2015;67(1):1-35. doi: 10.1124/pr.114.009225. PubMed PMID: 25287517.
54. Gonzalez P, Uhlinger KR, Lowe CJ. The Adult Body Plan of Indirect Developing Hemichordates Develops by Adding a Hox-Patterned Trunk to an Anterior Larval Territory. Current Biology. 2017;27(1):87-95. doi: https://doi.org/10.1016/j.cub.2016.10.047.
55. dos Reis M, Thawornwattana Y, Angelis K, Telford Maximilian J, Donoghue Philip CJ, Yang Z. Uncertainty in the Timing of Origin of Animals and the Limits of Precision in Molecular Timescales. Current Biology. 2015;25(22):2939-50. doi: https://doi.org/10.1016/j.cub.2015.09.066.
56. Gold DA, Runnegar B, Gehling JG, Jacobs DK. Ancestral state reconstruction of ontogeny supports a bilaterian affinity for Dickinsonia. Evolution & Development. 2015;17(6):315-24. doi: https://doi.org/10.1111/ede.12168.

57. Hedges SB, Marin J, Suleski M, Paymer M, Kumar S. Tree of Life Reveals Clock-Like Speciation and Diversification. Molecular biology and evolution. 2015;32(4):835-45. doi: 10.1093/molbev/msv037.
58. Wiemuth D, Assmann M, Grunder S. The bile acid-sensitive ion channel (BASIC), the ignored cousin of ASICs and ENaC. Channels (Austin). 2014;8(1):29-34. doi: 10.4161/chan.27493. PubMed PMID: 24365967; PubMed Central PMCID: PMCPMC4048340.
59. Wiemuth D, Grunder S. A single amino acid tunes Ca2+ inhibition of brain liver intestine Na+ channel (BLINaC). The Journal of biological chemistry. 2010;285(40):30404-10. doi: 10.1074/jbc.M110.153064. PubMed PMID: 20656685; PubMed Central PMCID: PMCPMC2945532.
60. Golubovic A, Kuhn A, Williamson M, Kalbacher H, Holstein TW, Grimmelikhuijzen CJ, et al. A peptide-gated ion channel from the freshwater polyp Hydra. The Journal of biological chemistry. 2007;282(48):35098-103. doi: 10.1074/jbc.M706849200. PubMed PMID: 17911098.
61. Paukert M, Sidi S, Russell C, Siba M, Wilson SW, Nicolson T, et al. A family of acid-sensing ion channels from the zebrafish: widespread expression in the central nervous system suggests a conserved role in neuronal communication. The Journal of biological chemistry. 2004;279(18):18783-91. doi: 10.1074/jbc.M401477200. PubMed PMID: 14970195.
62. Richter S, Loesel R, Purschke G, Schmidt-Rhaesa A, Scholtz G, Stach T, et al. Invertebrate neurophylogeny: suggested terms and definitions for a neuroanatomical glossary. Frontiers in Zoology. 2010;7(1):29. doi: 10.1186/1742-9994-7-29.
63. Krishtal OA, Pidoplichko VI. Receptor for protons in the membrane of sensory neurons. Brain research. 1981;214(1):150-4. doi: https://doi.org/10.1016/0006-8993(81)90446-7.
64. Kreple CJ, Lu Y, Taugher RJ, Schwager-Gutman AL, Du J, Stump M, et al. Acid-sensing ion channels contribute to synaptic transmission and inhibit cocaine-evoked plasticity. Nat Neurosci. 2014;17(8):1083-91. doi: 10.1038/nn.3750. PubMed PMID: 24952644; PubMed Central PMCID: PMCPMC4115047.
65. Rigon F, Gasparini F, Shimeld SM, Candiani S, Manni L. Developmental signature, synaptic connectivity and neurotransmission are conserved between vertebrate hair cells and tunicate coronal cells. Journal of Comparative Neurology. 2018;526(6):957-71. doi: https://doi.org/10.1002/cne.24382.
66. Storozhuk M, Kondratskaya E, Nikolaenko L, Krishtal O. A modulatory role of ASICs on GABAergic synapses in rat hippocampal cell cultures. Molecular brain. 2016;9(1):90. doi: 10.1186/s13041-016-0269-4.
67. Onoa B, Li H, Gagnon-Bartsch JA, Elias LAB, Edwards RH. Vesicular Monoamine and Glutamate Transporters Select Distinct Synaptic Vesicle Recycling Pathways. The Journal of Neuroscience. 2010;30(23):7917. doi: 10.1523/JNEUROSCI.5298-09.2010.
68. Dong X, Ko KH, Chow J, Tuo B, Barrett KE, Dong H. Expression of acid-sensing ion channels in intestinal epithelial cells and their role in the regulation of duodenal mucosal bicarbonate secretion. Acta Physiologica. 2011;201(1):97-107. doi: https://doi.org/10.1111/j.1748-1716.2010.02207.x.
69. Su X, Li Q, Shrestha K, Cormet-Boyaka E, Chen L, Smith PR, et al. Interregulation of Proton-gated Na+ Channel 3 and Cystic Fibrosis Transmembrane Conductance Regulator*. Journal of Biological Chemistry. 2006;281(48):36960-8. doi: https://doi.org/10.1074/jbc.M608002200.
70. Ustaoglu A, Sawada A, Lee C, Lei W-Y, Chen C-L, Hackett R, et al. Heartburn sensation in nonerosive reflux disease: pattern of superficial sensory nerves expressing TRPV1 and epithelial cells expressing ASIC3 receptors. American Journal of Physiology-Gastrointestinal and Liver Physiology. 2021;320(5):G804-G15. doi: 10.1152/ajpgi.00013.2021.
71. Diochot S, Baron A, Salinas M, Douguet D, Scarzello S, Dabert-Gay AS, et al. Black mamba venom peptides target acid-sensing ion channels to abolish pain. Nature. 2012;490(7421):552-5. doi: 10.1038/nature11494. PubMed PMID: 23034652.
72. Gu Q, Lee L-Y. Characterization of acid signaling in rat vagal pulmonary sensory neurons. American Journal of Physiology-Lung Cellular and Molecular Physiology. 2006;291(1):L58-L65. doi: 10.1152/ajplung.00517.2005.
73. Stolfi A, Ryan K, Meinertzhagen IA, Christiaen L. Migratory neuronal progenitors arise from the neural plate borders in tunicates. Nature. 2015;527(7578):371-4. doi: 10.1038/nature15758.

74. Albertin CB, Simakov O, Mitros T, Wang ZY, Pungor JR, Edsinger-Gonzales E, et al. The octopus genome and the evolution of cephalopod neural and morphological novelties. Nature. 2015;524(7564):220-4. doi: 10.1038/nature14668.
75. Fu H, Jiao Z, Li Y, Tian J, Ren L, Zhang F, et al. Transient Receptor Potential (TRP) Channels in the Pacific Oyster (Crassostrea gigas): Genome-Wide Identification and Expression Profiling after Heat Stress between C. gigas and C. angulata. International Journal of Molecular Sciences. 2021;22(6):3222. PubMed PMID: doi:10.3390/ijms22063222.
76. Simakov O, Marletaz F, Cho S-J, Edsinger-Gonzales E, Havlak P, Hellsten U, et al. Insights into bilaterian evolution from three spiralian genomes. Nature. 2013;493(7433):526-31. doi: 10.1038/nature11696.
77. Xun X, Cheng J, Wang J, Li Y, Li X, Li M, et al. Solute carriers in scallop genome: Gene expansion and expression regulation after exposure to toxic dinoflagellate. Chemosphere. 2020;241:124968. doi: https://doi.org/10.1016/j.chemosphere.2019.124968.
78. Zhang G, Fang X, Guo X, Li L, Luo R, Xu F, et al. The oyster genome reveals stress adaptation and complexity of shell formation. Nature. 2012;490(7418):49-54. doi: 10.1038/nature11413.
79. Howard RJ, Edgecombe GD, Shi X, Hou X, Ma X. Ancestral morphology of Ecdysozoa constrained by an early Cambrian stem group ecdysozoan. BMC Evolutionary Biology. 2020;20(1):156. doi: 10.1186/s12862-020-01720-6.
80. Schmidt-Rhaesa A, Bartolomaeus T, Lemburg C, Ehlers U, Garey JR. The position of the Arthropoda in the phylogenetic system. Journal of Morphology. 1998;238(3):263-85. doi: https://doi.org/10.1002/(SICI)1097-4687(199812)238:3<263::AID-JMOR1>3.0.CO;2-L.
81. Ringers C, Olstad EW, Jurisch-Yaksi N. The role of motile cilia in the development and physiology of the nervous system. Philosophical transactions of the Royal Society of London Series B, Biological sciences. 2020;375(1792):20190156. Epub 2019/12/31. doi: 10.1098/rstb.2019.0156. PubMed PMID: 31884916; PubMed Central PMCID: PMCPMC7017337.
82. Valentine JW, Collins AG. The significance of moulting in Ecdysozoan evolution. Evolution & Development. 2000;2(3):152-6. doi: https://doi.org/10.1046/j.1525-142x.2000.00043.x.
83. Shah Alok S, Ben-Shahar Y, Moninger Thomas O, Kline Joel N, Welsh Michael J. Motile Cilia of Human Airway Epithelia Are Chemosensory. Science. 2009;325(5944):1131-4. doi: 10.1126/science.1173869.
84. Andrikou C, Thiel D, Ruiz-Santiesteban JA, Hejnol A. Active mode of excretion across digestive tissues predates the origin of excretory organs. PLOS Biology. 2019;17(7):e3000408. doi: 10.1371/journal.pbio.3000408.
85. Katoh K, Standley DM. MAFFT Multiple Sequence Alignment Software Version 7: Improvements in Performance and Usability. Molecular biology and evolution. 2013;30(4):772-80. doi: 10.1093/molbev/mst010.
86. Guindon S, Dufayard J-F, Lefort V, Anisimova M, Hordijk W, Gascuel O. New Algorithms and Methods to Estimate Maximum-Likelihood Phylogenies: Assessing the Performance of PhyML 3.0. Systematic Biology. 2010;59(3):307-21. doi: 10.1093/sysbio/syq010.
87. Anisimova M, Gil M, Dufayard J-F, Dessimoz C, Gascuel O. Survey of Branch Support Methods Demonstrates Accuracy, Power, and Robustness of Fast Likelihood-based Approximation Schemes. Systematic Biology. 2011;60(5):685-99. doi: 10.1093/sysbio/syr041.
88. Shannon TR, Achatz JG. Convolutriloba macropyga sp. nov., an uncommonly fecund acoel (Acoelomorpha) discovered in tropical aquaria. Zootaxa. 2007;1525:1-17.
89. Smith JPSI, Bush L. Convoluta pulchra n. sp. (Turbellaria: Acoela) from the East Coast of North America. Transactions of the American Microscopical Society. 1991;110(1):12-26. doi: 10.2307/3226735.
90. De Mulder K, Kuales G, Pfister D, Willems M, Egger B, Salvenmoser W, et al. Characterization of the stem cell system of the acoel Isodiametra pulchra. BMC Developmental Biology. 2009;9(1):69. doi: 10.1186/1471-213X-9-69.
91. Correa D. Two new marine turbellaria from Florida. Bulletin of Marine Science. 1960;10(2):208-16.

92. Srivastava M, Mazza-Curll Kathleen L, van Wolfswinkel Josien C, Reddien Peter W. Whole-Body Acoel Regeneration Is Controlled by Wnt and Bmp-Admp Signaling. Current Biology. 2014;24(10):1107-13. doi: https://doi.org/10.1016/j.cub.2014.03.042.
93. Pixell HLM. Memoirs: two new species of the Phoronidea from Vancouver Island. Quarterly Journal of Microscopical Science. 1912;2(230):257-84.
94. Sowerby GB. Descriptions of thirteen new species of brachiopods. Proceedings of the Zoological Society of London. 1846:14:91-5.
95. Delle Chiaje S. Descrizione e notomia degli animali invertebrati della Sicilia citeriore osservati vivi negli anni 1822-1830. Batteli & Co, Naples. 1841:1-8.
96. Cameron CB, Perez M. Spengelidae (Hemichordata: Enteropneusta) from the Eastern Pacific including a new species, Schizocardium californicum, from California. Zootaxa. 2012;3569(1):79–88. doi: 10.11646/zootaxa.3569.1.6.
97. Freeman G. Metamorphosis in the Brachiopod Terebratalia: Evidence for a Role of Calcium Channel Function and the Dissociation of Shell Formation from Settlement. The Biological Bulletin. 1993;184(1):15-24. doi: 10.2307/1542376.
98. Gonzalez P, Jiang JZ, Lowe CJ. The development and metamorphosis of the indirect developing acorn worm Schizocardium californicum (Enteropneusta: Spengelidae). Frontiers in Zoology. 2018;15(1):26. doi: 10.1186/s12983-018-0270-0.
99. Rattenbury JC. The embryology of Phoronopsis viridis. Journal of Morphology. 1954;95(2):289-349. doi: https://doi.org/10.1002/jmor.1050950206.
100. Wilson DP. IV. On the Mitraria Larva of Owenia fusiformis Delle Chiaje. Philosophical transactions of the Royal Society of London Series B, Biological sciences. 1932;221:231-334. doi: 10.1098/rstb.1932.0004.
101. Jékely G, Arendt D. Cellular resolution expression profiling using confocal detection of NBT/BCIP precipitate by reflection microscopy. BioTechniques. 2007;42(6):751-5. doi: 10.2144/000112462.

Supplemental Files

S1 Fig. DEG/ENaC gene tree. Maximum likelihood tree of 700 DEG/ENaC amino acid sequences from 47 animals (using LG + G substitution model; see *Materials and Methods*, *Survey and phylogenetic analysis*). Branch support inferred by fast likelihood-based methods aLRT SH-like (expanded tree) and aBayes (compact tree). *Aaur = Aurelia aurita* (Cnidaria), *Agra = Acanthopleura granulata* (Mollusca), *Apla = Acanthaster planci* (Echinodermata), *Aque = Amphimedon queenslandica* (Porifera), *Bbel = Branchiostoma belcheri* (Chordata), *Bpli = Brachionus plicatilis* (Rotifera), *Cele = Caenorhabditis elegans* (Nematodea), *Cgig = Crassostrea gigas* (Mollusca), *Cmac = Convolutriloba macropyga* (Xenacoelomorpha), *Crob = Ciona robusta* (Chordata), *Cscu = Centruroides sculpturatus* (Arthropoda), *Csub = Childia submaculatum* (Xenacoelomorpha), *Dgig = Dendronephthya gigantea* (Cnidaria), *Dgyr = Dinophilus gyrociliatus* (Annelida), *Dmel = Drosophila melanogaster* (Arthropoda), *Dpul = Daphnia pulex* (Arthropoda), *Esen = Epiphanes senta* (Rotifera), *Hmia = Hofstenia miamia* (Xenacoelomorpha), *Hspi = Halicryptus spinulosus* (Priapulida), *Hvul = Hydra vulgaris* (Cnidaria), *Ipul = Isodiametra pulchra* (Xenacoelomorpha), *Lana = Lingula anatina* (Brachiopoda), *Llon = Lineus longissimus (Nemertea), Lsqu = Lepidodermella squamata (Gastrotricha), Lvir = Lineus viridis* (Nemertea), *Mlei = Mnemiopsis leidyi* (Ctenophora), *Mmem = Membranipora membranacea* (Bryozoa), *Msti = Meara stichopi* (Xenacoelomorpha), *Nano = Novocrania anomala* (Brachiopoda), *Ngen = Notospermus geniculatus* (Nemertea), *Nvec = Nematostella vectensis* (Cnidaria), *Nwes = Nemertoderma westbladi* (Xenacoelomorpha), *Odio = Oikopleura dioica* (Chordata), *Ofus = Owenia fusiformis* (Annelida), *Pbac = Pleurobranchia bachei* (Ctenophora), *Pcau = Priapulus caudatus* (Priapulida), *Pfla = Ptychodera flava* (Hemichordata), *Phar = Phoronopsis harmeri* (Phoronida), *Pvit = Prostheceraeus vittatus* (Platyhelminthes), *Pvul = Pontonema vulgare* (Nematoda), *Rnor = Rattus norvegicus* (Chordata), *Scal = Schizocardium californicum* (Hemichordata), *Smed = Schmidtea mediterranea* (Platyhelminthes), *Spad = Spadella sp* (Chaetognatha), *Ttra = Terebratalia transversa* (Brachiopoda), *Xboc = Xenoturbella bocki* (Xenacoelomorpha), *Xpro = Xenoturbella profunda* (Xenacoelomorpha). Reponses to increased proton concentrations at oocytes expressing channels closely related to ASICs are shown: heterotrimeric cnidarian HyNaC (pink); rat BASIC (orange). Other ligands are the peptide Hydra-RFamide-I ((pE)WLGGRFamide; pE, pyroglutamate) and the bile acid sodium ursodeoxycholic acid (NaUDCA).

S1 Text. Amino acid sequence alignment of 700 DEG/ENaC genes from 47 species. Details described in *Materials and Methods, Survey and phylogenetic analysis*).

S2 Text. Modified pSP64 vector and ASIC inserts.